

**Supplementary Information to "Effects of bariatric surgery on functional connectivity of the reward and default mode network: a pre-registered analysis"**

Hannah Sophie Heinrichs <sup>1,\*</sup> and Frauke Beyer <sup>1,2,\*</sup>

<sup>1</sup>Max-Planck-Institute for Human Cognitive and Brain Sciences, Leipzig

<sup>2</sup>CRC 1052 "Obesity Mechanisms", Subproject A1, University of Leipzig

\*The authors contributed equally.

## Supplementary Information to "Effects of bariatric surgery on functional connectivity of the reward and default mode network: a pre-registered analysis"

### Methods

#### Sample

Table 1 shows the distribution of data points in the present rsfMRI study, for the bariatric surgery group (BARS) and the waiting-list control group (NBARS).

Table 1

*Distribution of data points at months after intervention*

	BARS	NBARS
count: only 0	7	2
count: only 6	3	0
count: only 12	2	0
count: 0 and 6	4	3
count: 6 and 12	7	1
count: complete data	10	9
total number of subjects	33	15
total data points	64	37

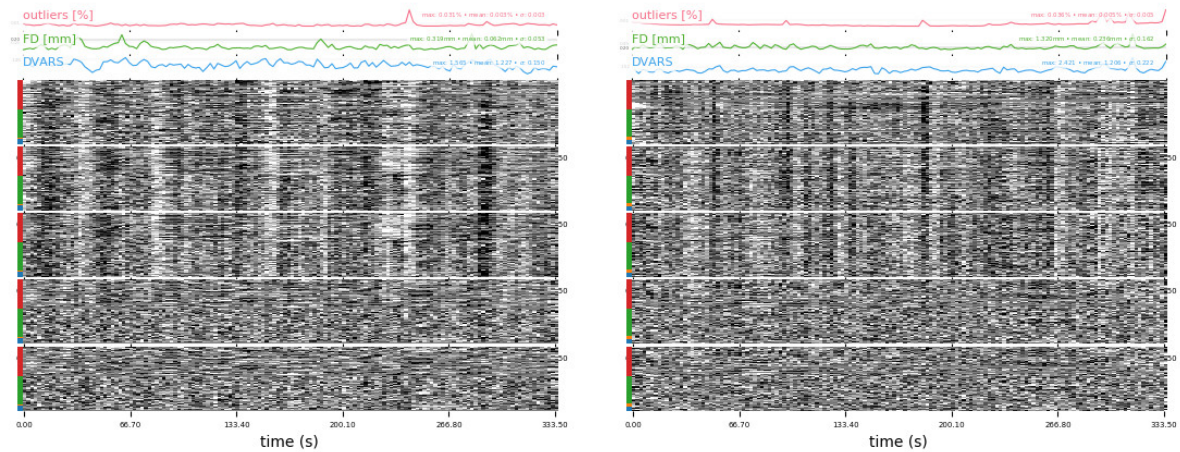
#### Denoising Pipelines

We pre-registered two distinct denoising pipelines which were previously shown to efficiently remove motion artifacts in fMRI. In Parkes et al., 2018, ICA-AROMA provided an acceptable trade-off between the mitigation of motion-FC correlation and the introduction of a distance-dependence on motion-FC relationship. Ciric et al., 2017 showed that GSR is very efficient in removing the correlation of head motion and FC, and outperforms ICA-AROMA alone. Yet, it introduces spatial dependency and spurious correlations.

**ICA-AROMA denoising pipeline.** As described in Pruim et al., 2015, the minimally preprocessed data underwent independent component analysis (ICA) using FSL’s `melodic` and nuisance components were classified according to four spectral and spatial criteria. Finally, the timeseries of the nuisance components were regressed from the raw rsfMRI timeseries non-aggressively. As recommended in the original paper, we performed regression of WM and CSF signal on the ICA-AROMA result. We used CompCor to estimate 5 variance components from a combined WM and CSF mask, which was further eroded using `fslmaths -nan -thr 0.99 -ero -bin` Behzadi et al., 2007; Muschelli et al., 2014. After regression of these nuisance components from the data, we performed high-pass filtering at 0.01 Hz.

**Global Signal Regression (GSR).** The global signal was derived from the average of all voxels in the brain mask. Then, we regressed WM and CSF CompCor components along with the GS from the ICA-AROMA rsfMRI data and high-pass filtered the resulting file as above.

## Quality Control



(a) Example 1 with strong amount of structured noise

(b) Example 2 with less amount of structured noise

Figure 1. Carpet plot for quality control

**Individual level rsfMRI QC.** On the individual level, we used `plot_carpet` from `niworkflows.viz.plots` to generate carpet plots which depict denoising quality.

Figure 1 shows an exemplary carpet plot with (from top to bottom): percent outliers

defined by AFNI, mFD, `OutlierCount`, DVARS (spatial root mean square of the data after temporal differencing), voxelwise timeseries from minimally preprocessed, AROMA non-aggressive and aggressive denoising, CC and CC + GSR data (red: GM voxels, green: WM voxels, blue: ventricle, green: cerebellum). All carpet plots were visually checked and if there was still structured noise in the CC+GSR-denoised functional data (such as black/white stripes, signal dropout), the participant was given a rating of 1 in `QA residuals`, and checked again visually. No participant was excluded based on this visual inspection.

**Group level rsfMRI QC.** As described in Beyer et al., 2020, there was a group-by-time interaction on mFD (see Figure 2, upper right panel). The intervention group reduced in head motion in the followup assessments compared to the control group. For this study, we further explored mFD and its relation to DVARS, the root mean square of the temporal change of the voxel-wise signal at each time point. DVARS measures volume-to-volume signal variation. DVARS did not qualitatively differ between groups and time points, and the correlation of DVARS and mFD remained similar over time points (see Figure S2 in supplements). To further assess the confounding of head motion and FC, we evaluated mFD-FC relationships by computing a functional connectome based on the protocol by Ciric et al., 2018. We used the MNI coordinates of 246 cortical and subcortical spherical seed regions from Power et al., 2012 with 5mm radius in `NiftiSpheresMasker`, and calculated the Spearman rank correlation between these time series. Then, we calculated the distance-dependence of mFD-FC correlations by correlating the euclidean distance between nodes with the mFD-QC correlation.

In the minimally preprocessed data, mFD and FC between nodes were significantly positively correlated (mean Spearman's  $r = 0.07$ ) (see Table 2). This relationship was negatively associated with distance between nodes (mean Spearman's  $r = -0.29$ ). Denoising pipelines (AROMA, AROMA+CC, AROMA+CC+GSR) gradually reduced the correlation of mFD and FC, and reduced the distance dependency. Contrary to previous reports, GSR did not exacerbate mFD-FC distance dependency Power et al.,

Table 2  
Summary of quality metrics

	mean mFD-FC	median mFD-FC	sig. conn.	sig. conn. BH	mean distance- mFDFC	$p_{dist}$
minimally processed	0.072	0.071	7349	1571	-0.292	< 0.0001
AROMA	0.061	0.063	4854	20	-0.021	0.0001
AROMA + CC	0.034	0.037	5756	237	0.062	< 0.0001
AROMA + CC + GSR	0.006	0.010	5838	407	0.069	< 0.0001

mean mFD-FC, mean Spearman's correlation of mFD and FC; median mFD-FC, median Spearman's correlation of mFD and FC; sig. conn., number of significant connections; sig. conn. BH, number of FDR-corrected, significant connections; mean distance-mFDFC, mean Spearman's correlation of distance and mFD-FC correlation;  $p_{dist}$ , p-value of distance dependency)

2015. Overall, AROMA+CC+GSR performed best, with almost no mFD-FC correlation (mean Spearman's  $r = 0.01$ ), and minimal positive distance dependence (mean Spearman's  $r = 0.07$ ) In addition, for models showing a significant time-by-group interaction, we planned to perform a sensitivity analysis excluding the 10% data sets with highest mFD.

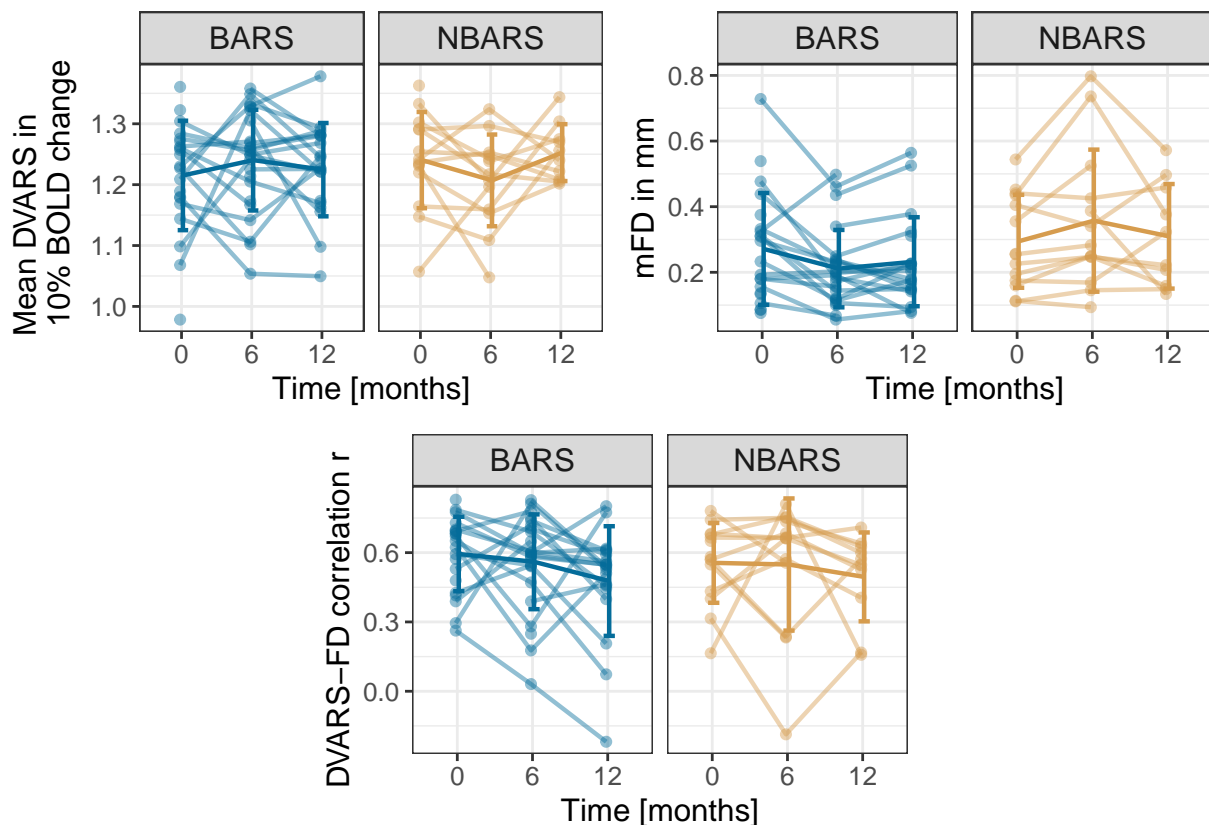


Figure 2. Summary of quality measures DVARS, mFD and their correlation

Figure 3 shows the distribution of FC-QC correlations for minimally preprocessed, AROMA, AROMA+CC and AROMA+CC+GSR preprocessed data. With more

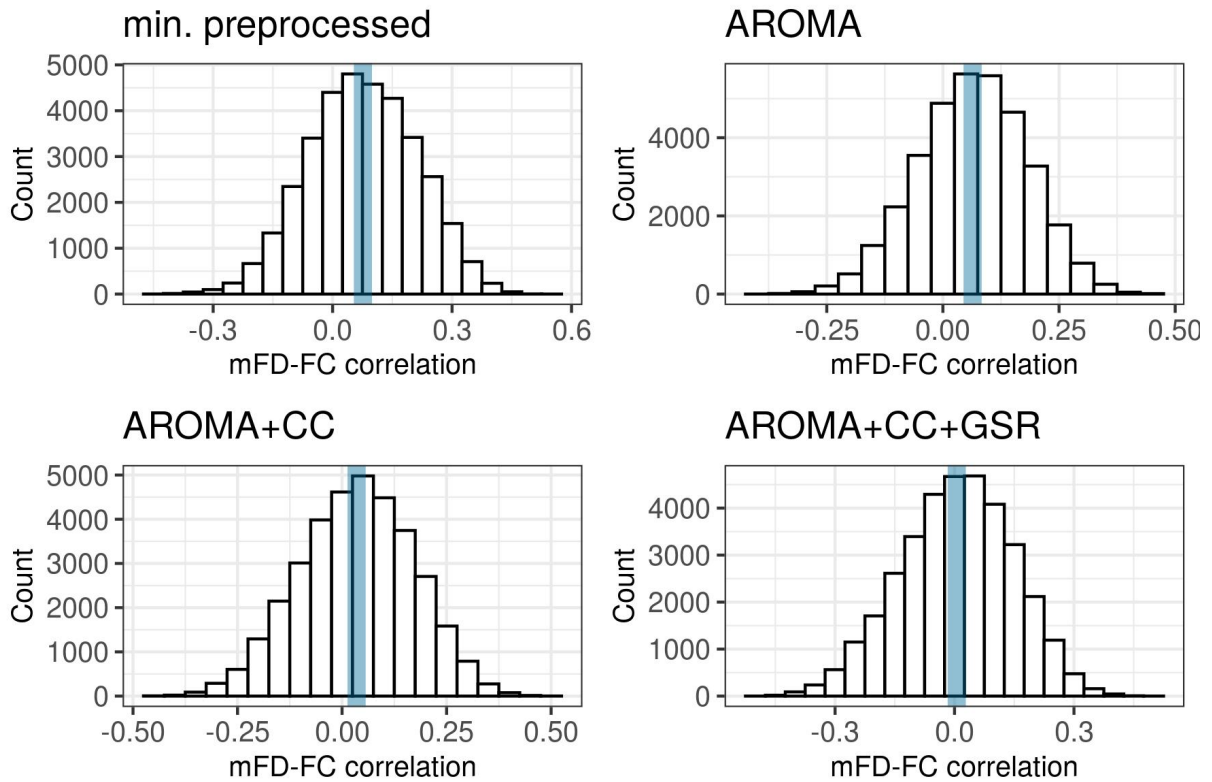


Figure 3. Histograms of FC-QC correlations for different denoising pipelines)

denoising, there is a decreasing number of high correlations between FC and the measure of head motion, supporting the positive effect of denoising.

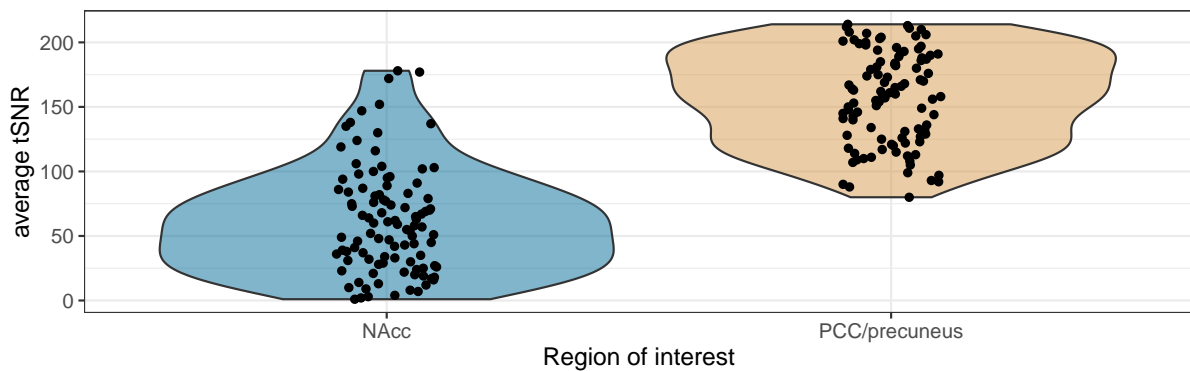
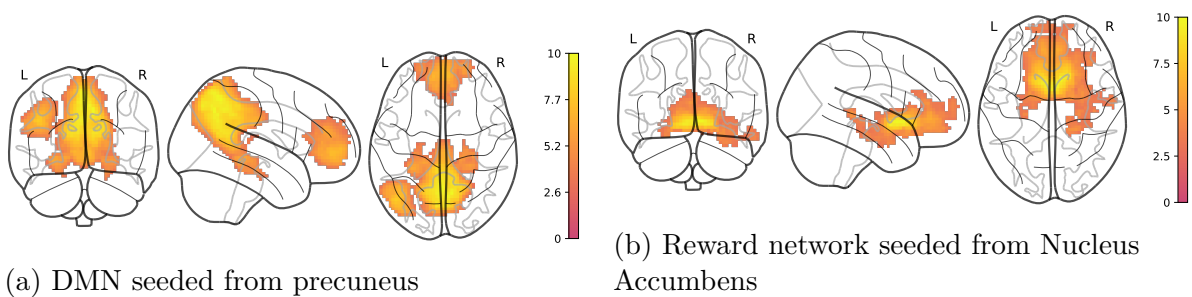


Figure 4. Lower tSNR in the region of interest NAcc versus precuneus used for seed-based connectivity (shown are all 101 time points)

## DMN and RN Networks

Figure 5 shows the DMN and reward network average maps which we used for extracting aggregated FC values. Both networks included the typically described brain

regions (i.e. medial prefrontal cortex, parietal lobules and posterior hippocampus for the DMN, and anterior cingulate, right amygdala and ventromedial-prefrontal cortex for the reward network). Yet, the reward network was less pronounced (overall lower T-values) and less symmetric (no significant connectivity with left amygdala), which might be due to lower SNR in the seeded brain region (see 4). Unthresholded maps for the t-tests of the DMN and reward network (which were used for data aggregation) are on Neurovault.



*Figure 5.* Resting state networks based on AROMA+CC+GSR input data, one-sample t-tests adjusting for age and sex over all time points and participants with bootstrapped clusterwise inference (FWE-corrected  $p < 0.05$ ). Legend denotes empirical Z-values.

## Statistical analysis

For our confirmatory analysis on the model CA3 adjusting age, sex, average logmFD and baseline BMI, one participant in the intervention group had no baseline BMI. In order to make full use of the data available, we employed multivariate imputation, using the package `mice` based on subject identification, condition, baseline age, and available BMI values to obtain a reasonable estimate for the missing baseline BMI. The package allows taking into account the multi-level structure of the data and averaging across multiple possible values, in this case 50 different values, each derived from 10 iterations. Figure 6 illustrates the design matrix used for the confirmatory analyses (regressors for confounders not depicted).

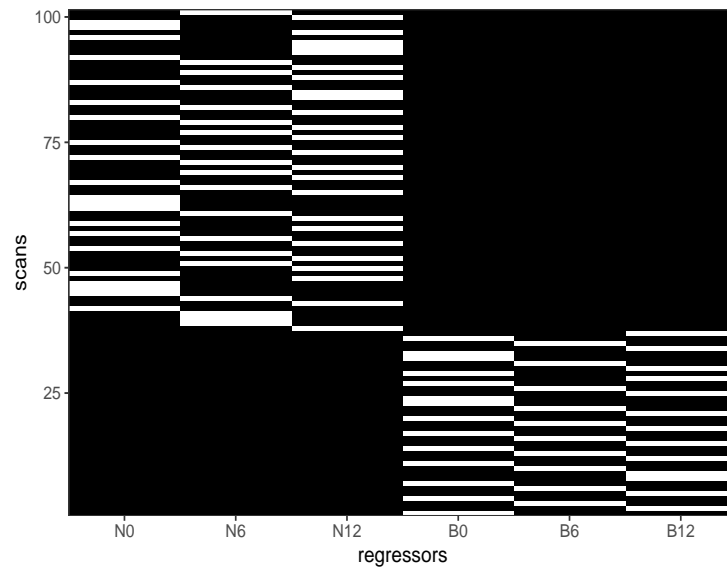


*Figure 6.* Design matrices of time-by-group model with time as categorical factor. N, NBARS; B, BARS; numbers indicate month of measurement since beginning, 0 indicates baseline(pre-surgery measurement, 6 and 12 indicate months after baseline/surgery.

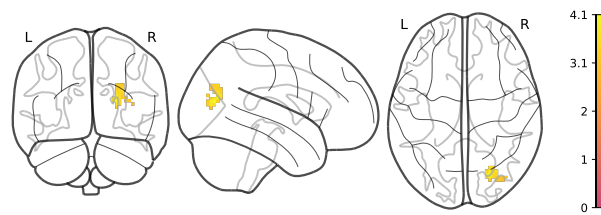


*Figure 7.* Main effect of time: Negative Association of FC between NAcc and this cluster in lateral parietal cortex, adjusted for age, sex, avgFD, and baseline BMI in AROMA+CC+GSR preprocessed data. Legend denotes empirical Z-values.

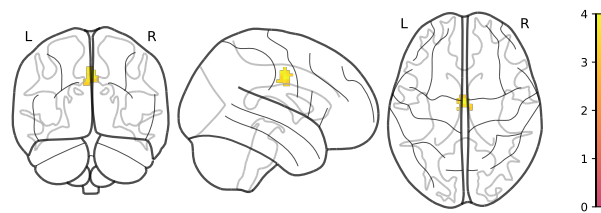


*Figure 8.* Main effect of time: Negative Association of FC between PCC/precuneus and this cluster in ACC, adjusted for age, sex, avgFD, and baseline BMI in AROMA+CC+GSR preprocessed data. Legend denotes empirical Z-values.

## Results

### Whole brain analysis: group-by-time interaction effect

### Aggregated FC: group-by-time interaction effect

**Reward network.** Illustration of empirical trajectories and results from mixed-models with aggregated FC in Table 3 to 5 for two time points and Table 6 to 8.



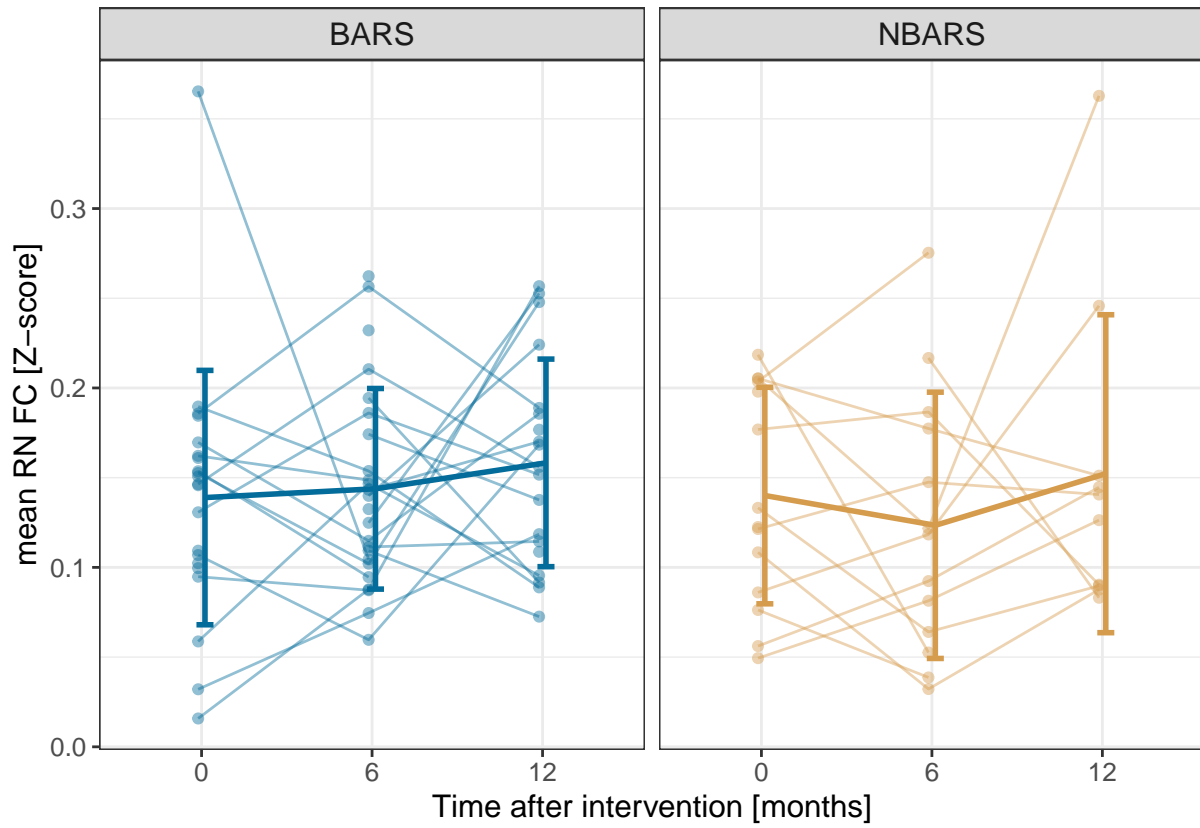


Table 3  
Two time points, without adjustments (model CA1)

	R0	R1
Intercept (BL, NBARS)	0.136 (0.015)***	0.142 (0.017)***
Timepoint FU	−0.006 (0.013)	−0.018 (0.021)
Group BARS	0.009 (0.017)	−0.000 (0.022)
Timepoint x Group		0.019 (0.027)
AIC	−165.366	−158.506
Log Likelihood	87.683	85.253
Num. obs.	72	72
Num. groups: subj.ID	46	46
Var: subj.ID (Intercept)	0.001	0.001
Var: Residual	0.003	0.003

Standard deviation is shown in brackets.

\*\*\* $p < 0.001$ ; \*\* $p < 0.01$ ; \* $p < 0.05$

**DMN.** Illustration of empirical trajectories and results from mixed-models with aggregated FC in Table 9 to 11 for two time points and Table 12 to 11.

Table 4

*Two time points, adjusted for age, sex and average logmFD (model CA2)*

	R0	R1
Intercept (BL, NBARS)	0.082 (0.056)	0.091 (0.057)
Timepoint FU	−0.007 (0.014)	−0.018 (0.021)
Group BARS	0.007 (0.019)	−0.003 (0.024)
Timepoint x Group		0.019 (0.028)
Age	0.001 (0.001)	0.001 (0.001)
Sex	−0.003 (0.011)	−0.004 (0.011)
av logmFD	−0.035 (0.043)	−0.035 (0.043)
AIC	−136.181	−129.321
Log Likelihood	76.090	73.660
Num. obs.	72	72
Num. groups: subj.ID	46	46
Var: subj.ID (Intercept)	0.001	0.001
Var: Residual	0.003	0.003

Standard deviation is shown in brackets.

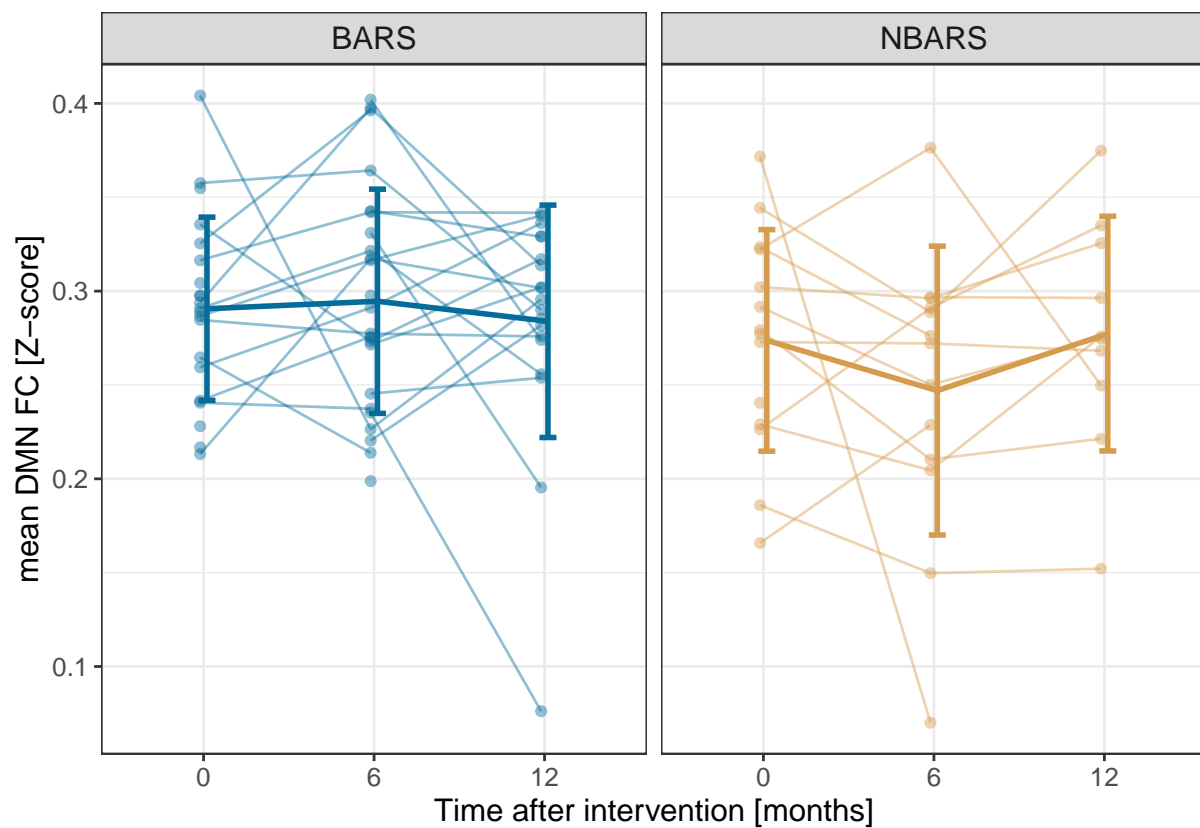
\*\*\* $p < 0.001$ ; \*\* $p < 0.01$ ; \* $p < 0.05$ 

Table 5

*Two time points, adjusted for age, sex, average of logmFD and baseline BMI (model CA3)*

	R0	R1
Intercept (BL, NBARS)	0.039 (0.091)	0.055 (0.094)
Timepoint FU	−0.009 (0.014)	−0.018 (0.021)
Group BARS	0.005 (0.019)	−0.003 (0.024)
Timepoint x Group		0.017 (0.028)
Age	0.001 (0.001)	0.001 (0.001)
Sex	−0.002 (0.011)	−0.003 (0.011)
av logmFD	−0.035 (0.044)	−0.034 (0.044)
baseline BMI	0.001 (0.002)	0.001 (0.002)
AIC	−123.570	−116.611
Log Likelihood	70.785	68.305
Num. obs.	72	72
Num. groups: subj.ID	46	46
Var: subj.ID (Intercept)	0.001	0.001
Var: Residual	0.003	0.003

Standard deviation is shown in brackets.

\*\*\* $p < 0.001$ ; \*\* $p < 0.01$ ; \* $p < 0.05$

### Exploratory Analyses: Effects of average and change BMI on FC

**Reward network.** Find the results from all mixed-models with aggregated FC in Table 15 and Table 16.

**DMN.** Find the results from all mixed-models with aggregated FC in Table 17 and Table 18.

**Anatomical Labelling for models.** Find in the detailed Output of the SPM Anatomy toolbox, version 2.2c. For Clusters without any labels, the toolbox was unable to assign any grey matter area. Models evaluated were model EA1 estimating the effects of average BMI and change in BMI, adjusting for age and sex (Table 19), then model EA2 where we additionally adjusted for logmFD (Table 20), and model EA3 estimating the effects of average BMI and BMI variability as well as average logmFD and change in logmFD, adjusting for age and sex (Table 21 to Table 25). Last, the FD model estimating the unique effects of average logmFD and change in logmFD when adjusting for age and sex was evaluated (Table 26 and Table 27).

Table 6

*Three time points, without adjustments (model CA1)*

	R0	R1
Intercept (BL, NBARS)	0.135 (0.014)***	0.140 (0.018)***
Timepoint FU	−0.004 (0.015)	−0.016 (0.024)
Timepoint FU2	0.017 (0.016)	0.013 (0.026)
Group BARS	0.009 (0.015)	−0.001 (0.023)
Timepoint FU x Group		0.020 (0.031)
Timepoint FU2 x Group		0.007 (0.033)
AIC	−228.437	−214.503
Log Likelihood	120.218	115.251
Num. obs.	101	101
Num. groups: subj.ID	48	48
Var: subj.ID (Intercept)	0.001	0.001
Var: Residual	0.004	0.004

Standard deviation is shown in brackets.

\*\*\* $p < 0.001$ ; \*\* $p < 0.01$ ; \* $p < 0.05$ 

Table 7

*Three time points, adjusted for age, sex and average logmFD (model CA2)*

	R0	R1
Intercept (BL, NBARS)	0.089 (0.047)	0.097 (0.049)*
Timepoint FU	−0.004 (0.015)	−0.017 (0.024)
Timepoint FU2	0.018 (0.016)	0.013 (0.026)
Group BARS	0.005 (0.016)	−0.006 (0.024)
Timepoint FU x Group		0.022 (0.031)
Timepoint FU2 x Group		0.009 (0.033)
Age	0.000 (0.001)	0.000 (0.001)
Sex	−0.005 (0.009)	−0.006 (0.009)
av logmFD	−0.037 (0.037)	−0.037 (0.037)
AIC	−199.069	−185.215
Log Likelihood	108.535	103.607
Num. obs.	101	101
Num. groups: subj.ID	48	48
Var: subj.ID (Intercept)	0.001	0.001
Var: Residual	0.004	0.004

Standard deviation is shown in brackets.

\*\*\* $p < 0.001$ ; \*\* $p < 0.01$ ; \* $p < 0.05$

Table 8

*Three time points, adjusted for age, sex, average of logmFD and baseline BMI (model CA3)*

	R0	R1
Intercept (BL, NBARS)	0.087 (0.074)	0.101 (0.077)
Timepoint FU	−0.004 (0.015)	−0.017 (0.024)
Timepoint FU2	0.018 (0.016)	0.013 (0.026)
Group BARS	0.004 (0.016)	−0.006 (0.024)
Timepoint FU x Group		0.022 (0.031)
Timepoint FU2 x Group		0.009 (0.034)
Age	0.000 (0.001)	0.000 (0.001)
Sex	−0.005 (0.009)	−0.006 (0.009)
av logmFD	−0.037 (0.038)	−0.037 (0.038)
baseline BMI	0.000 (0.001)	−0.000 (0.001)
AIC	−185.697	−171.888
Log Likelihood	102.849	97.944
Num. obs.	101	101
Num. groups: subj.ID	48	48
Var: subj.ID (Intercept)	0.001	0.001
Var: Residual	0.004	0.004

Standard deviation is shown in brackets.

\*\*\* $p < 0.001$ ; \*\* $p < 0.01$ ; \* $p < 0.05$

Table 9

*Two time points, without adjustments (model CA1)*

	R0	R1
Intercept (BL, NBARS)	0.265 (0.014)***	0.274 (0.016)***
Timepoint FU	−0.008 (0.014)	−0.027 (0.022)
Group BARS	0.032 (0.015)*	0.016 (0.021)
Timepoint x Group		0.032 (0.028)
AIC	−172.192	−166.152
Log Likelihood	91.096	89.076
Num. obs.	72	72
Num. groups: subj.ID	46	46
Var: subj.ID (Intercept)	0.000	0.000
Var: Residual	0.003	0.003

Standard deviation is shown in brackets.

\*\*\* $p < 0.001$ ; \*\* $p < 0.01$ ; \* $p < 0.05$

Table 10

*Two time points, adjusted for age, sex and average logmFD (model CA2)*

	R0	R1
Intercept (BL, NBARS)	0.262 (0.049)***	0.277 (0.051)***
Timepoint FU	−0.006 (0.014)	−0.027 (0.022)
Group BARS	0.029 (0.016)	0.011 (0.022)
Timepoint x Group		0.036 (0.028)
Age	−0.000 (0.001)	−0.000 (0.001)
Sex	−0.007 (0.009)	−0.008 (0.010)
av logmFD	−0.005 (0.038)	−0.004 (0.038)
AIC	−141.808	−136.102
Log Likelihood	78.904	77.051
Num. obs.	72	72
Num. groups: subj.ID	46	46
Var: subj.ID (Intercept)	0.000	0.001
Var: Residual	0.003	0.003

Standard deviation is shown in brackets.

\*\*\* $p < 0.001$ ; \*\* $p < 0.01$ ; \* $p < 0.05$ 

Table 11

*Two time points, adjusted for age, sex, average of logmFD and baseline BMI (model CA3)*

	R0	R1
Intercept (BL, NBARS)	0.330 (0.081)***	0.367 (0.084)***
Timepoint FU	−0.002 (0.015)	−0.028 (0.022)
Group BARS	0.032 (0.017)	0.010 (0.022)
Timepoint x Group		0.043 (0.029)
Age	−0.000 (0.001)	−0.000 (0.001)
Sex	−0.009 (0.010)	−0.010 (0.010)
av logmFD	−0.006 (0.038)	−0.005 (0.038)
baseline BMI	−0.002 (0.001)	−0.002 (0.001)
AIC	−129.742	−124.723
Log Likelihood	73.871	72.361
Num. obs.	72	72
Num. groups: subj.ID	46	46
Var: subj.ID (Intercept)	0.000	0.000
Var: Residual	0.003	0.003

Standard deviation is shown in brackets.

\*\*\* $p < 0.001$ ; \*\* $p < 0.01$ ; \* $p < 0.05$

Table 12

*Three time points, without adjustments (model CA1)*

	R0	R1
Intercept (BL, NBARS)	0.268 (0.014)***	0.275 (0.016)***
Timepoint FU	−0.006 (0.013)	−0.028 (0.020)
Timepoint FU2	−0.005 (0.014)	−0.001 (0.022)
Group BARS	0.024 (0.015)	0.012 (0.021)
Timepoint FU x Group		0.036 (0.026)
Timepoint FU2 x Group		−0.006 (0.028)
AIC	−246.374	−234.237
Log Likelihood	129.187	125.119
Num. obs.	101	101
Num. groups: subj.ID	48	48
Var: subj.ID (Intercept)	0.001	0.001
Var: Residual	0.003	0.003
Standard deviation is shown in brackets.		
*** $p < 0.001$ ; ** $p < 0.01$ ; * $p < 0.05$		

Table 13

*Three time points, adjusted for age, sex and average logmFD (model CA2)*

	R0	R1
Intercept (BL, NBARS)	0.268 (0.046)***	0.280 (0.048)***
Timepoint FU	−0.003 (0.013)	−0.028 (0.020)
Timepoint FU2	−0.003 (0.014)	−0.000 (0.022)
Group BARS	0.020 (0.016)	0.006 (0.022)
Timepoint FU x Group		0.040 (0.026)
Timepoint FU2 x Group		−0.003 (0.028)
Age	−0.000 (0.001)	−0.000 (0.001)
Sex	−0.010 (0.009)	−0.011 (0.009)
av logmFD	−0.007 (0.036)	−0.006 (0.037)
AIC	−216.912	−205.185
Log Likelihood	117.456	113.592
Num. obs.	101	101
Num. groups: subj.ID	48	48
Var: subj.ID (Intercept)	0.001	0.001
Var: Residual	0.003	0.003
Standard deviation is shown in brackets.		
*** $p < 0.001$ ; ** $p < 0.01$ ; * $p < 0.05$		

Table 14

*Three time points, adjusted for age, sex, average of logmFD and baseline BMI (model CA3)*

	R0	R1
Intercept (BL, NBARS)	0.373 (0.069)***	0.399 (0.072)***
Timepoint FU	0.000 (0.013)	−0.029 (0.020)
Timepoint FU2	0.001 (0.014)	−0.002 (0.022)
Group BARS	0.027 (0.015)	0.007 (0.021)
Timepoint FU x Group		0.048 (0.026)
Timepoint FU2 x Group		0.008 (0.029)
Age	−0.000 (0.001)	−0.000 (0.001)
Sex	−0.012 (0.009)	−0.013 (0.009)
av logmFD	−0.010 (0.035)	−0.009 (0.035)
baseline BMI	−0.003 (0.001)*	−0.003 (0.001)*
AIC	−207.304	−196.179
Log Likelihood	113.652	110.090
Num. obs.	101	101
Num. groups: subj.ID	48	48
Var: subj.ID (Intercept)	0.001	0.001
Var: Residual	0.003	0.003

Standard deviation is shown in brackets.

\*\*\* $p < 0.001$ ; \*\* $p < 0.01$ ; \* $p < 0.05$

Table 15

*Model EA1 (without adjustment) and EA2 (adjusting for logmFD)*

	R0	R1
Intercept	0.164 (0.063)**	0.118 (0.073)
average BMI	−0.001 (0.001)	−0.001 (0.001)
change BMI	−0.001 (0.002)	−0.001 (0.002)
Age	0.000 (0.001)	0.001 (0.001)
Sex	−0.009 (0.008)	−0.006 (0.009)
logmFD		−0.040 (0.032)
AIC	−203.135	−197.692
Log Likelihood	108.568	106.846
Num. obs.	101	101
Num. groups: subj.ID	48	48
Var: subj.ID (Intercept)	0.000	0.000
Var: Residual	0.004	0.004

Standard deviation is shown in brackets.

\*\*\* $p < 0.001$ ; \*\* $p < 0.01$ ; \* $p < 0.05$



Table 16

*Model EA3 (adjusting for average and change in logmFD)*

	R1
Intercept	0.123 (0.075)
average BMI	−0.001 (0.001)
change BMI	−0.000 (0.002)
average logmFD	−0.036 (0.036)
change logmFD	−0.059 (0.071)
Age	0.000 (0.001)
Sex	−0.006 (0.009)
AIC	−192.543
Log Likelihood	105.271
Num. obs.	101
Num. groups: subj.ID	48
Var: subj.ID (Intercept)	0.000
Var: Residual	0.004
Standard deviation is shown in brackets.	
*** $p < 0.001$ ; ** $p < 0.01$ ; * $p < 0.05$	

Table 17

*Model EA1 (without adjustment) and EA2 (adjusting for logmFD)*

	R0	R1
Intercept	0.423 (0.060)***	0.397 (0.070)***
average BMI	−0.003 (0.001)*	−0.003 (0.001)*
change BMI	−0.000 (0.001)	0.000 (0.002)
Age	−0.000 (0.001)	−0.000 (0.001)
Sex	−0.013 (0.008)	−0.012 (0.008)
logmFD		−0.023 (0.030)
AIC	−227.166	−220.547
Log Likelihood	120.583	118.274
Num. obs.	101	101
Num. groups: subj.ID	48	48
Var: subj.ID (Intercept)	0.001	0.001
Var: Residual	0.003	0.003
Standard deviation is shown in brackets.		
*** $p < 0.001$ ; ** $p < 0.01$ ; * $p < 0.05$		

Table 18

*Model EA3 (adjusting for average and change in logmFD)*

	R1
Intercept	0.413 (0.073)***
average BMI	−0.003 (0.001)*
change BMI	0.001 (0.002)
average logmFD	−0.009 (0.034)
change logmFD	−0.064 (0.059)
Age	−0.000 (0.001)
Sex	−0.013 (0.008)
AIC	−215.664
Log Likelihood	116.832
Num. obs.	101
Num. groups: subj.ID	48
Var: subj.ID (Intercept)	0.001
Var: Residual	0.003
Standard deviation is shown in brackets.	
*** $p < 0.001$ ; ** $p < 0.01$ ; * $p < 0.05$	

Table 19

*Anatomical labels for clusters functionally connected to the PCC showing a negative association with average BMI in model EA1 on AROMA+CC denoised data.*

Cluster	Number of voxels in cluster	% of cluster volume assigned	Hemisphere	Area	% of area overlap with cluster
Cluster 1 (212 voxel)	5.5	2.6	left	Lobule I IV (Hem)	3.3
	2.6	1.2	right	Area hOc1 [V1]	0.4
	1.4	0.7	left	Lobule V (Hem)	0.6
	0.7	0.3	right	Area hOc2 [V2]	0.2
	0.4	0.2	left	Thal: Prefrontal	0.2
	0.4	0.2	left	Subiculum	0.3
	0.2	0.1	right	Subiculum	0.2
	0.2	0.1	left	Thal: Parietal	0.2
	0.1	0.1	left	Area hOc1 [V1]	0.0
	11.5	5.4		assigned in total	
Cluster 2 (77 voxel)	21.8	28.3	right	Area TE 3	7.1
	21.8	28.3		assigned in total	
Cluster 3 (75 voxel)	37.1	49.5	left	Area Fp2	17.3
	25.9	34.5	right	Area Fp2	14.3
	1.6	2.2	left	Area s32	2.6
	0.6	0.7	right	Area Fp1	0.1
	65.1	86.9		assigned in total	
Cluster 4 (70 voxel)	4.1	5.9	left	Area TE 3	1.6
	0.6	0.8	left	Area Id1	1.6
	4.7	6.7		assigned in total	

Table 20

*Anatomical labels for clusters functionally connected to the PCC showing a negative association with average BMI in model EA2 on AROMA+CC denoised data.*

Cluster	Number of voxels in cluster	% of cluster volume assigned	Hemisphere	Area	% of area overlap with cluster
Cluster 1 (230 voxel)					
	5.5	2.4	left	Lobule I IV (Hem)	3.3
	2.6	1.1	right	Area hOc1 [V1]	0.4
	1.6	0.7	left	Lobule V (Hem)	0.6
	1.6	0.7	left	Thal: Prefrontal	0.7
	0.7	0.3	left	Thal: Visual	2.4
	0.7	0.3	right	Area hOc2 [V2]	0.2
	0.5	0.2	left	Thal: Parietal	0.5
	0.4	0.2	left	Subiculum	0.3
	0.2	0.1	right	Subiculum	0.2
	0.1	0.1	left	Area hOc1 [V1]	0.0
	13.9	6.0		assigned in total	
Cluster 2 (76 voxel)					
	37.8	49.8	left	Area Fp2	17.6
	28.4	37.4	right	Area Fp2	15.7
	0.1	0.1	left	Area s32	0.1
	66.3	87.2		assigned in total	
Cluster 3 (70 voxel)					
	4.1	5.9	left	Area TE 3	1.6
	0.3	0.4	left	Area Id1	0.9
	4.4	6.3		assigned in total	
Cluster 4 (67 voxel)					
	18.1	27.0	right	Area TE 3	5.9
	18.1	27.0		assigned in total	

Table 21

*Anatomical labels for clusters functionally connected to the NAcc showing a negative association with change in BMI in model EA3 on AROMA+CC denoised data.*

Cluster	Number of voxels in cluster	% of cluster volume assigned	Hemisphere	Area	% of area overlap with cluster
Cluster 1 (112 voxel)					

Table 22

*Anatomical labels for clusters functionally connected to the NAcc showing a positive association with average mFD in model EA3 on AROMA+CC denoised data.*

Cluster	Number of voxels in cluster	% of cluster volume assigned	Hemisphere	Area	% of area overlap with cluster
Cluster 1 (143 voxel)					
	12.9	9.0	right	Area 4a	4
	0.1	0.1	left	Area 4a	0
	13.0	9.1		assigned in total	

Table 23

*Anatomical labels for clusters functionally connected to the NAcc showing a negative association with change in BMI in model EA3 on AROMA+CC+GSR denoised data.*

Cluster	Number of voxels in cluster	% of cluster volume assigned	Hemisphere	Area	% of area overlap with cluster
Cluster 1 (99 voxel)					

Table 24

*Anatomical labels for clusters functionally connected to the NAcc showing a positive association with average mFD in model EA3 on AROMA+CC+GSR denoised data.*

Cluster	Number of voxels in cluster	% of cluster volume assigned	Hemisphere	Area	% of area overlap with cluster
Cluster 1 (99 voxel)					

Table 25

*Anatomical labels for clusters functionally connected to the PCC showing a negative association with average BMI in model EA3 on AROMA+CC denoised data.*

Cluster	Number of voxels in cluster	% of cluster volume assigned	Hemisphere	Area	% of area overlap with cluster
Cluster 1 (251 voxel)					
	6.0	2.4	left	Lobule I IV (Hem)	3.7
	4.6	1.8	left	Thal: Parietal	4.3
	2.7	1.1	right	Area hOc1 [V1]	0.4
	2.2	0.9	left	Lobule V (Hem)	0.9
	1.8	0.7	left	Subiculum	1.4
	1.6	0.6	left	Thal: Prefrontal	0.7
	0.7	0.3	right	Area hOc2 [V2]	0.2
	0.7	0.3	left	Thal: Visual	2.4
	0.2	0.1	right	Subiculum	0.2
	0.1	0.1	left	Area hOc1 [V1]	0.0
	20.5	8.2		assigned in total	
Cluster 2 (91 voxel)					
	42.0	46.2	left	Area Fp2	19.6
	32.9	36.1	right	Area Fp2	18.1
	1.6	1.8	left	Area s32	2.6
	76.5	84.1		assigned in total	
Cluster 3 (70 voxel)					
	4.1	5.9	left	Area TE 3	1.6
	0.3	0.4	left	Area Id1	0.9
	4.4	6.3		assigned in total	
Cluster 4 (69 voxel)					
	19.8	28.7	right	Area TE 3	6.4
	19.8	28.7		assigned in total	

Table 26

*Anatomical labels for clusters functionally connected to the NAcc showing a positive association with average mFD in model EA6 on AROMA+CC denoised data.*

Cluster	Number of voxels in cluster	% of cluster volume assigned	Hemisphere	Area	% of area overlap with cluster
Cluster 1 (126 voxel)					
	5.6	4.5	right	Area 4a	1.7
	5.6	4.5		assigned in total	

Table 27

*Anatomical labels for clusters functionally connected to the NAcc showing a positive association with average mFD in model EA6 on AROMA+CC denoised data.*

Cluster	Number of voxels in cluster	% of cluster volume assigned	Hemisphere	Area	% of area overlap with cluster
Cluster 1 (126 voxel)	5.6	4.5	right	Area 4a	1.7
	5.6	4.5		assigned in total	

## References

- Behzadi, Y., Restom, K., Liau, J., & Liu, T. T. (2007). A component based noise correction method (CompCor) for BOLD and perfusion based fMRI. *NeuroImage*, *37*(1), 90–101. <https://doi.org/10.1016/j.neuroimage.2007.04.042>
- Beyer, F., Prehn, K., Wüsten, K. A., Villringer, A., Ordemann, J., Flöel, A., & Witte, A. V. (2020). Weight loss reduces head motion: Revisiting a major confound in neuroimaging. *Human Brain Mapping*, *41*(9), 2490–2494. <https://doi.org/10.1002/hbm.24959>
- Ciric, R., Rosen, A. F. G., Erus, G., Cieslak, M., Adebimpe, A., Cook, P. A., Bassett, D. S., Davatzikos, C., Wolf, D. H., & Satterthwaite, T. D. (2018). Mitigating head motion artifact in functional connectivity MRI. *Nature Protocols*, *13*(12), 2801–2826. <https://doi.org/10.1038/s41596-018-0065-y>
- Ciric, R., Wolf, D. H., Power, J. D., Roalf, D. R., Baum, G. L., Ruparel, K., Shinohara, R. T., Elliott, M. A., Eickhoff, S. B., Davatzikos, C., Et al. (2017). Benchmarking of participant-level confound regression strategies for the control of motion artifact in studies of functional connectivity. *NeuroImage*, *154*, 174–187. <https://doi.org/10.1016/j.neuroimage.2017.03.020>
- Muschelli, J., Nebel, M. B., Caffo, B. S., Barber, A. D., Pekar, J. J., & Mostofsky, S. H. (2014). Reduction of motion-related artifacts in resting state fMRI using aCompCor. *NeuroImage*, *96*, 22–35. <https://doi.org/10.1016/j.neuroimage.2007.04.042>
- Parkes, L., Fulcher, B., Yücel, M., & Fornito, A. (2018). An evaluation of the efficacy, reliability, and sensitivity of motion correction strategies for resting-state functional MRI. *NeuroImage*, *171*, 415–436. <https://doi.org/10.1016/j.neuroimage.2017.12.073>
- Power, J. D., Barnes, K. A., Snyder, A. Z., Schlaggar, B. L., & Petersen, S. E. (2012). Spurious but systematic correlations in functional connectivity MRI networks arise from subject motion. *NeuroImage*, *59*(3), 2142–2154. <https://doi.org/10.1016/j.neuroimage.2011.10.018>

- Power, J. D., Schlaggar, B. L., & Petersen, S. E. (2015). Recent progress and outstanding issues in motion correction in resting state fmri. *Neuroimage*, *105*, 536–551.
- Pruim, R. H. R., Mennes, M., van Rooij, D., Llera, A., Buitelaar, J. K., & Beckmann, C. F. (2015). Ica-aroma: A robust ica-based strategy for removing motion artifacts from fmri data. *Neuroimage*, *112*, 267–277.